Technische Universität Chemnitz
Sonderforschungsbereich 393
Numerische Simulation auf massiv parallelen Rechnern

Helmut Harbrecht Reinhold Schneider

Wavelet Galerkin Schemes for Boundary Integral Equations – Implementation and Quadrature

Preprint SFB393/02-21

Preprint-Reihe des Chemnitzer SFB 393
ISSN 1619-7178 (Print) **ISSN 1619-7186** (Internet)

SFB393/02-21 **October 2002**

Contents

Author's addresses:

Helmut Harbrecht and Reinhold Schneider
TU Chemnitz
Fakultät für Mathematik
D-09107 Chemnitz

http://www.tu-chemnitz.de/sfb393/

Abstract

In this paper we consider the fully discrete wavelet Galerkin scheme for the fast solution of boundary integral equations in three dimensions. It produces approximate solutions within discretization error accuracy offered by the underlying Galerkin method at a computational expense that stays proportional to the number of unknowns. We focus on implementational details of the scheme, in particular on numerical integration of relevant matrix coefficients. We illustrate the proposed algorithms by numerical results.

AMS Subject Classification: 47A20, 65F10, 65F50, 65N38, 65R20
Key Words: Boundary integral equations, biorthogonal wavelet bases, matrix compression, numerical integration.

Introduction

Various problems in science and engineering can be formulated as boundary integral equations. In general, boundary integral equations are solved numerically by the boundary element method (BEM). For example, BEM is a favourable approach for the treatment of exterior boundary value problems. Nevertheless, traditional discretizations of integral equations suffer from a major disadvantage. The associated system matrices are densely populated. Therefore, the complexity for solving such equations is at least $\mathcal{O}(N_J^2)$, where N_J denotes the number of equations. This fact restricts the maximal size of the linear equations seriously.

Modern methods for the fast solution of BEM reduce the complexity to a suboptimal rate, i.e., $\mathcal{O}(N_J \log^\alpha N_J)$, or even an optimal rate, i.e., $\mathcal{O}(N_J)$. Prominent examples for such methods are the *fast multipole method* [16], the *panel clustering* [17] or the *wavelet Galerkin scheme* [1, 6, 10, 11, 29]. In fact, a Galerkin discretization with wavelet bases results in quasi-sparse matrices, i.e., the most matrix entries are negligible and can be treated as zero. Discarding these nonrelevant matrix entries is called matrix compression. It has been shown in [6, 29] that only $\mathcal{O}(N_J)$ significant matrix entries remain.

Concerning boundary integral equations, a strong effort has been spent on the construction of appropriate wavelet bases on surfaces [8, 12, 13, 19, 24, 29]. In order to achieve the optimal complexity of the wavelet Galerkin scheme, wavelet bases are required with a sufficiently large number of vanishing moments. Our realization is based on biorthogonal spline wavelets derived from the multiresolution developed in [3]. These wavelets are advantageous since the regularity of the duals is known [31]. Moreover, the duals are compactly supported which preserves the linear complexity of the fast wavelet transform also for its inverse. This is an important task for the coupling of FEM and BEM, cf. [20, 21]. Additionally, in view of the discretization of operators of positive order, for instance, the hypersingular operator, globally continuous wavelets are available [2, 4, 12, 19].

The efficient computation of the relevant matrix coefficients turned out to be an important task for the successful application of the wavelet Galerkin method [19, 25, 29]. We present a fully discrete Galerkin scheme based on numerical quadrature. Supposing that the given manifold is piecewise analytic we can use a hp-quadrature scheme [19, 29, 30] in combination with exponentially convergent quadrature rules. This yields an algorithm with asymptotically linear complexity without compromising the accuracy of the Galerkin scheme.

The outline of the present paper is as follows. First, in Section 1, we introduce the class of problems under consideration. Then, in Section 2 we provide the wavelet bases on manifolds an recall the matrix compression in Section 3. The next sections are concerned with implementational aspects: In Section 4 a suitable data structure is introduced to handle a wide class of wavelets, in Section 5 the numerical evaluation of distances is performed, in Section 7 the computation of the compressed system matrix is reduced to the computation of certain element-element interactions which are investigated in Section 8. Section 9 is concerned with the quadrature of element-element interactions which correspond mostly to nearly singular and singular integrals. We prove that our quadrature strategy computes the compressed system matrix within linear complexity. In Section 10 we present numerical results which confirm our analysis quite well. The accuracy of the Galerkin scheme is never compromised by the matrix compression.

1 Problem formulation and preliminaries

We consider boundary integral equations on a closed boundary surface Γ of a three dimensional domain $\Omega \subset \mathbb{R}^3$

$$Au = f \quad \text{on } \Gamma, \tag{1}$$

where the boundary integral operator

$$Au(x) = \int_\Gamma k(x,y)u(y)d\Gamma_y$$

is assumed to be an operator of order $2q$, that is

$$A : H^q(\Gamma) \to H^{-q}(\Gamma).$$

The kernel functions under consideration are supposed to be smooth as functions in the variables x, y, apart from the diagonal $\{(x,y) \in \Gamma \times \Gamma : x = y\}$ and may have a singularity on the diagonal. Such kernel functions arise, for instance, by applying a boundary integral formulation to a second order elliptic problem. In general, they decay like a negative power of the distance of the arguments which depends on the order $2q$ of the operator.

Throughout the remainder of this paper we shall assume that the boundary manifold Γ is given as a parametric surface consisting of smooth patches. More precisely, let $\square := [0,1]^2$ denote the unit square. The manifold $\Gamma \in \mathbb{R}^3$ is partitioned into a finite number of *patches*

$$\Gamma = \bigcup_{i=1}^M \Gamma_i, \qquad \Gamma_i = \gamma_i(\square), \qquad i = 1, 2, \ldots, M, \tag{2}$$

where each $\gamma_i : \square \to \Gamma_i$ defines a diffeomorphism of $\square$ onto Γ_i. The intersection $\Gamma_i \cap \Gamma_{i'}$, $i \neq i'$, of the patches Γ_i and $\Gamma_{i'}$ is supposed to be either empty or a common edge or vertex.

A mesh of level j on Γ is induced by dyadic subdivisions of depth j of the unit square into 4^j squares

$$\square_{j,k} = [2^{-j}k_1, 2^{-j}(k_1+1)] \times [2^{-j}k_2, 2^{-j}(k_2+1)] \subseteq \square,$$

where $k = (k_1, k_2)$ with $0 \le k_1, k_2 < 2^j$. This generates 4^{jM} *elements* (or elementary domains) $\Gamma_{i,j,k} := \gamma_i(\square_{j,k}) \subseteq \Gamma_i$, $i = 1, \ldots, M$.

In order to ensure that the collection of elements $\{\Gamma_{i,j,k}\}$ on the level j forms a regular mesh on Γ, the parametric representation is subjected to the following *matching condition*: For all $x \in \Gamma_i \cap \Gamma_{i'}$ exists a bijective, affine mapping $\Xi : \square \to \square$ such that $\gamma_i(s) = (\gamma_{i'} \circ \Xi)(s) = x$ for $s = (s_1, s_2) \in \square$ with $\gamma_i(s) = x$. A conforming mesh of a gearwheel is depicted in Figure 1.

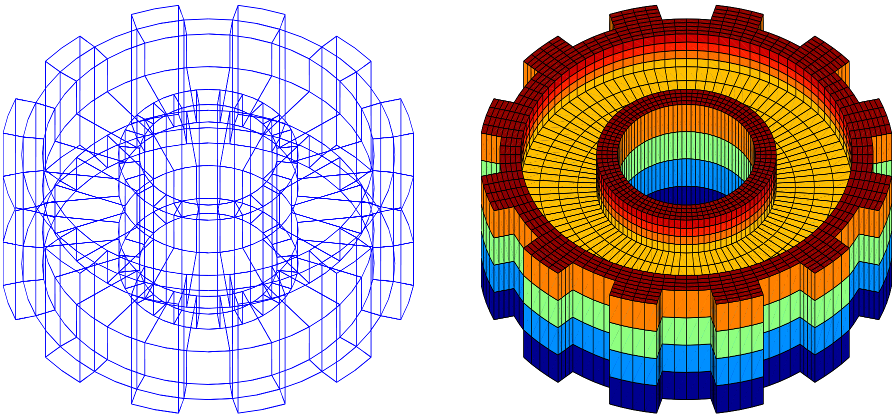

Figure 1: A gearwheel represented by 336 patches (left) and the resulting mesh on the level 2 (right).

Denoting the surface measure by $\kappa_i(s) := \|\partial_{s_1}\gamma_i(s) \times \partial_{s_2}\gamma_i(s)\|$, the canonical inner product in $L^2(\Gamma)$ is given by

$$\langle u, v\rangle := \int_\Gamma u(x)v(x)d\Gamma_x = \sum_{i=1}^{M} \int_\square u\big(\gamma_i(s)\big)v\big(\gamma_i(s)\big)\kappa_i(s)ds.$$

The corresponding Sobolev spaces are denoted by $H^t(\Gamma)$, endowed with the norms $\|\cdot\|_t$, where for $t < 0$ it is understood that $H^t(\Gamma) = (H^{-t}(\Gamma))'$. Of course, depending on the global smoothness of the surface, the range of permitted $t \in \mathbb{R}$ is limited to $s \in (-t_\Gamma, t_\Gamma)$.

In the sequel it will be rather convenient to have access to the *local parametrizations* $\gamma_{i,j,k} : \square \to \Gamma_{i,j,k}$ given by

$$\gamma_{i,j,k}(s) := \gamma_i\big(2^{-j}\left[\begin{smallmatrix} k_1+s_1 \\ k_2+s_2 \end{smallmatrix}\right]\big), \qquad s = \left[\begin{smallmatrix} s_1 \\ s_2 \end{smallmatrix}\right] \in \square. \tag{3}$$

For $m \in \mathbb{N}$ we conclude

$$\partial_{s_n}^m \gamma_{i,j,k}(s) = 2^{-jm}\ \partial_{s_n}^m \gamma_i\big(2^{-j}\left[\begin{smallmatrix} k_1+s_1 \\ k_2+s_2 \end{smallmatrix}\right]\big), \qquad n = 1,2, \tag{4}$$

in particular, the corresponding surface measure satisfies

$$\kappa_{i,j,k}(s) := \big\|\partial_{s_1}\gamma_{i,j,k}(s) \times \partial_{s_2}\gamma_{i,j,k}(s)\big\| = 2^{-2j}\kappa_i\big(2^{-j}\left[\begin{smallmatrix} k_1+s_1 \\ k_2+s_2 \end{smallmatrix}\right]\big). \tag{5}$$

We can now specify the kernel functions. To this end, we denote by $\alpha = (\alpha_1, \alpha_2)$ and $\beta = (\beta_1, \beta_2)$ multi-indices of dimension two and define $|\alpha| := \alpha_1 + \alpha_2$.

Definition 1.1. *A kernel $k(x, y)$ is called standard kernel of order $2q$, if the partial derivatives of the transported kernel functions*

$$k_{i,i}(s, t) := k\big(\gamma_i(s), \gamma_{i'}(t)\big)\kappa_i(s)\kappa_{i'}(t), \tag{6}$$

$1 \le i, i' \le M$, are bounded by

$$|\partial_s^\alpha \partial_t^\beta k_{i,i}(s, t)| \lesssim \|\gamma_i(s), \gamma_{i'}(t)\|^{-(2+2q+|\alpha|+|\beta|)},$$

provided that $2 + 2q + |\alpha| + |\beta| > 0$.

We emphasize that this definition requires patchwise smoothness but *not* global smoothness of the geometry. The surface itself needs to be only Lipschitz. Generally, under this assumption, the kernel of a boundary integral operator A of order $2q$ is a standard kernel of order $2q$. Hence, we may assume this property in the sequel. We shall encounter further specifications in connection with numerical integration.

2 Biorthogonal wavelet bases

The nested trial spaces $V_j \subset V_{j+1}$ that we shall employ in the Galerkin scheme are the spaces of piecewise constant or bilinear functions on the given partition. These trial spaces have the *approximation order* $d = 1$ and $d = 2$ in the case of the piecewise constants and bilinears, respectively, i.e.

$$\inf_{v_j \in V_j} \|v - v_j\|_0 \lesssim 2^{-jd}\|v\|_d.$$

These trial space are spanned by so called *single-scale bases* $\Phi_j = \{\phi_{j,k} : k \in \Delta_j\}$ which can be specified as follows: On the level j, we find for each element $\Gamma_{i',j,k'}$ a piecewise constant scaling function $\phi_{j,k}$ with

$$\phi_{j,k}\big|_{\Gamma_{i',j,k'}} \equiv 2^j \tag{7}$$

and $\phi_{j,k}(x) = 0$ elsewhere. To describe the canonical piecewise bilinear scaling functions, we define four bilinear shape functions on the unit square

$$\begin{aligned} p_1^\square(s) &:= (1 - s_1)(1 - s_2), \qquad & p_2^\square(s) &:= s_1(1 - s_2), \\ p_3^\square(s) &:= s_1 s_2, & p_4^\square(s) &:= (1 - s_1)s_2. \end{aligned} \tag{8}$$

Then, $\phi_{j,k}$ is equal to 1 in one knot and equal to zero in the remaining knots and, if its support contains an element $\Gamma_{(i',j,k')}$, we find a $m \in \{1,2,3,4\}$ such that

$$\phi_{j,k}\big|_{\Gamma_{i',j,k'}}(x) = p_m^{\Box}(s), \qquad x = \gamma_{i',j,k'}(s) \in \Gamma_{i',j,k'}. \tag{9}$$

Continuity is supposed on each patch, but along the interfaces of the patches we may consider double knots or continuity. Notice that our definition yields the L^2-normalization $\|\phi_{j,k}\|_0 \sim 1$.

Associated with the *multiresolution sequence* $\{V_j\}_{j\geq j_0}$ is always a *dual* multiresolution sequence $\{\widetilde{V}_j\}_{j\geq j_0}$ which is generated by dual bases $\widetilde{\Phi}_j = \{\widetilde{\phi}_{j,k} : k \in \Delta_j\}$, i.e., one has $\langle \phi_{j,k}, \widetilde{\phi}_{j,k'}\rangle = \delta_{k,k'}$, $k,k' \in \Delta_j$. Here and below j_0 always stands for some fixed coarsest level of resolution that may depend on Γ. For the current type of boundary surfaces Γ the $\Phi_j, \widetilde{\Phi}_j$ are generated by constructing first dual pairs of single-scale bases on the interval $[0,1]$, using the dual components from [3] adapted to the interval [9]. Tensor products yield corresponding dual pairs on $\Box$. Using the parametric liftings γ_i and gluing across patch boundaries leads to globally continuous single-scale bases $\Phi_j, \widetilde{\Phi}_j$ on Γ [2, 4, 13, 19]. The dual spaces have approximation order $\widetilde{d} \geq d$ such that $d + \widetilde{d}$ is even.

Given the single-scale bases $\Phi_j, \widetilde{\Phi}_j$, one can construct now biorthogonal *complement bases* $\Psi_j = \{\psi_{j,k} : k \in \nabla_j\}$, $\widetilde{\Psi}_j = \{\widetilde{\psi}_{j,k} : k \in \nabla_j\}$, i.e., $\langle \psi_{j,k}, \widetilde{\psi}_{j',k'}\rangle = \delta_{(j,k),(j',k')}$, such that

$$\operatorname{diam}\operatorname{supp}\psi_{j,k} \sim \operatorname{diam}\operatorname{supp}\widetilde{\psi}_{j,k} \sim 2^{-j}, \quad j \geq j_0,$$

see e.g. [2, 4, 12, 13] and [19] for particularly useful local representations of important construction ingredients. We suppose these complement bases normalized in $L^2(\Gamma)$.

A biorthogonal or *dual* pair of wavelet bases is now obtained by taking the coarse single-scale basis and the union of the complement bases

$$\Psi = \bigcup_{j\geq j_0-1} \Psi_j, \qquad \widetilde{\Psi} = \bigcup_{j\geq j_0-1} \widetilde{\Psi}_j,$$

where we have set for convenience $\Psi_{j_0-1} := \Phi_{j_0}$, $\widetilde{\Psi}_{j_0-1} := \widetilde{\Phi}_{j_0}$. Of course, in the infinite dimensional case the notion of basis has to be made more specific. The key feature of the wavelet basis is now the fact that $\Psi, \widetilde{\Psi}$ are actually *Riesz bases* in $L^2(\Gamma)$.

From biorthogonality and the fact that the dual spaces $\widetilde{V}_j$ have the approximation order $\widetilde{d}$ one infers *vanishing moments* or the *cancellation property* of the primal wavelets

$$|\langle v, \psi_{j,k}\rangle| \lesssim 2^{-j(\widetilde{d}+1)} |v|_{W^{\widetilde{d},\infty}(\operatorname{supp}\psi_{j,k})}. \tag{10}$$

Here $|v|_{W^{\widetilde{d},\infty}(\Omega)} := \sup_{|\alpha|=\widetilde{d},\, x\in\Omega} |\partial^\alpha v(x)|$ denotes the semi-norm in $W^{\widetilde{d},\infty}(\Omega)$. The fact, that the concept of biorthogonality allows us to choose the order $\widetilde{d}$ of vanishing moments higher than the approximation order d, is essential for deriving optimal compression strategies that could not be realized by orthonormal bases.

3 Matrix compression

We shall be concerned with the Galerkin method for the solution of the given boundary integral equation (1): find $u_J \in V_J$ solving the variational problem

$$\langle Au_J, v_J\rangle = \langle f, v_J\rangle \quad \text{for all} \quad v_J \in V_J.$$

Traditionally this equation is discretized by the single-scale basis of V_J which yields a densely populated system matrix. Using instead wavelets with a sufficiently strong cancellation property (10), the system matrix becomes quasi-sparse and the most matrix coefficients are neglectable without compromising the order of convergence of the Galerkin scheme [6, 29].

But before we formulate this result, we introduce the following abbreviation

$$\Omega_{j,k} := \operatorname{conv\,hull}(\operatorname{supp}\psi_{j,k}), \qquad \Omega'_{j,k} := \operatorname{sing\,supp}\psi_{j,k}. \tag{11}$$

Notice that the first expression denotes the convex hull of the support of a wavelet whereas the second indicates its *singular support*, i.e. that subset of Γ where the wavelet is not smooth.

Theorem 3.1 (A-priori compression). *Let $\Omega_{j,k}$ and $\Omega'_{j,k}$ be given as in* (11) *and define the compressed system matrix $\mathbf{A}_J$, corresponding to the boundary integral operator A, by*

$$[\mathbf{A}_J]_{(j,k),(j',k')} := \begin{cases} 0, & \operatorname{dist}(\Omega_{j,k}, \Omega_{j',k'}) > \mathcal{B}_{j,j'} \text{ and } j, j' \geq j_0, \\ 0, & \operatorname{dist}(\Omega_{j,k}, \Omega_{j',k'}) \lesssim 2^{-\min\{j,j'\}} \text{ and} \\ & \operatorname{dist}(\Omega'_{j,k}, \Omega_{j',k'}) > \mathcal{B}'_{j,j'} \text{ if } j' > j \geq j_0 - 1, \\ & \operatorname{dist}(\Omega_{j,k}, \Omega'_{j',k'}) > \mathcal{B}'_{j,j'} \text{ if } j > j' \geq j_0 - 1, \\ \langle A\psi_{j',k'}, \psi_{j,k}\rangle, & \text{otherwise.} \end{cases} \tag{12}$$

Fixing

$$a, a' > 1, \qquad d < d' < \tilde{d} + 2q, \tag{13}$$

the cut-off parameters $\mathcal{B}_{j,j'}$ and $\mathcal{B}'_{j,j'}$ are set as follows

$$\begin{aligned} \mathcal{B}_{j,j'} &= a \max\left\{2^{-\min\{j,j'\}}, 2^{\frac{2J(d'-q)-(j+j')(d'+\tilde{d})}{2(\tilde{d}+q)}}\right\}, \\ \mathcal{B}'_{j,j'} &= a' \max\left\{2^{-\max\{j,j'\}}, 2^{\frac{2J(d'-q)-(j+j')d'-\max\{j,j'\}\tilde{d}}{\tilde{d}+2q}}\right\}. \end{aligned} \tag{14}$$

Then, the error estimate

$$\|u - u_J\|_{2q-d} \lesssim 2^{-2J(d-q)}\|u\|_d \tag{15}$$

holds for the solution u_J of the compressed Galerkin system provided that u and Γ is sufficiently regular.

In [6, 19] we presented a general theorem which shows that the overall complexity of assembling the compressed system matrix can be kept of the order $\mathcal{O}(N_J)$, $N_J = \dim V_J$, even when a computational cost of logarithmic order is allowed for each entry. This theorem will be used later as the essential ingredient in proving that the quadrature strategy proposed in Section 9 scales linearly.

Theorem 3.2. *Assume that $\mathbf{A}_J$ is compressed according to* (12). *The complexity of computing this compressed matrix is $\mathcal{O}(N_J)$ provided that for some $\alpha \geq 0$ at most $\mathcal{O}\big(\big[J - \frac{j+j'}{2}\big]^\alpha\big)$ operations are spent on the approximate calculation of the nonvanishing entries $\langle A\psi_{j',k'}, \psi_{j,k}\rangle$.*

Numerical integration of relevant matrix coefficients has to be performed with sufficient accuracy. In accordance with [6, 19] we can formulate a sufficient condition to retain the optimal order of convergence of the Galerkin scheme.

Theorem 3.3. *Let the matrix $\mathbf{A}_J$ denote the compressed system matrix according to Theorem 3.1 and consider the perturbed system matrix $\widetilde{\mathbf{A}}_J$ satisfying*

$$\big|[\mathbf{A}_J - \widetilde{\mathbf{A}}_J]_{(j,k),(j',k')}\big| \leq \varepsilon_{j,j'}$$

for all coefficients, where the level dependent error $\varepsilon_{j,j'}$ is given by

$$\varepsilon_{j,j'} \sim \min\Big\{2^{-|j-j'|}, 2^{-2(J-\frac{j+j'}{2})\frac{d'-q}{\tilde{d}+q}}\Big\} 2^{2Jq} 2^{-2d'(J-\frac{j+j'}{2})} \tag{16}$$

with $d' \in (d, \tilde{d} + 2q)$ from (13). *Then, the solution u_J of the perturbed Galerkin system satisfies* (15) *provided that u and Γ is sufficiently regular.*

If the order q of the boundary integral operator A is $\neq 0$, the compressed system matrix $\mathbf{A}_J$ becomes more and more ill conditioned when J increases. However, as a consequence of the norm equivalences of wavelet bases, the diagonally scaled system matrix has uniformly bounded spectral condition numbers, provided that the regularity $\tilde{\gamma}$ of the dual wavelets satisfies $\tilde{\gamma} > -q$ [5, 7, 10, 29].

4 The data structure

In general the wavelet bases are not simply defined via tensor products of the univariate case. In particular, considering globally continuous wavelets, a single wavelet might be supported on several patches. This requires a suitable data structure to handle such wavelet bases. The crucial idea is to split the support of a given wavelet into a set of elements which correspond to its smooth parts. Then, it suffices to store some additional weight factors in order to describe the wavelets uniquely. Moreover, it is convenient to arrange elements and wavelets in trees.

4.1 The element tree

According to Section 1 the elements $\Gamma_{i,j,k} = \gamma_i(\square_{j,k})$ are the images of the refined unit square under the parametric liftings γ_i. We introduce a hierarchical element tree with respect to "$\subseteq$" as follows. Starting with the M patches $\Gamma_i := \Gamma_{i,0,(0,0)}$ as the first generation, each element $\Gamma_{i,j,k}$ has the four sons $\Gamma_{i,j+1,k'} \subseteq \Gamma_{i,j,k}$, $k' \in \big\{(2k_1, 2k_2), (2k_1+1, 2k_2), (2k_1+1, 2k_2+1), (2k_1, 2k_2+1)\big\}$. Denoting by J the level of discretization, the tree consists of $J+1$ generations. The resulting tree is presented in Figure 2.

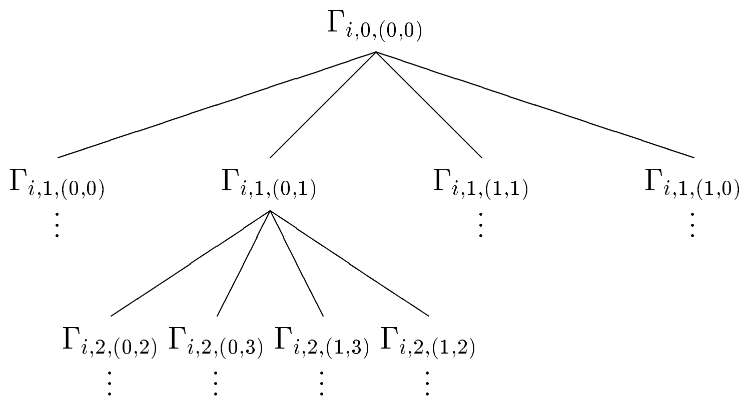

Figure 2: The hierarchical element tree to the elements $\{\Gamma_{i,j,k}\}$.

Notice that this element tree is given implicitly. The number of all elements is given by $N_\Gamma := \frac{N}{3}(4^{J+1} - 1)$. Hence, we may utilize the mapping

$$\lambda := \theta(i,j,k) = \frac{N}{3}(4^j - 1) + 4^j N i + 2^j k_2 + k_1 \tag{17}$$

to indicate the element $\Gamma_{i,j,k}$ uniquely by an integer $\lambda \in \{0, 1, \ldots, N_\Gamma - 1\}$. This numbering corresponds to indexing the element tree line-by-line. For a given index λ, the topological index (i,j,k) is calculated successively by

$$j = \Big\lfloor \log_4\Big(\tfrac{3\lambda}{N} + 1\Big)\Big\rfloor, \qquad i = \Big\lfloor \tfrac{\lambda - \frac{N}{3}(4^j - 1)}{4^j}\Big\rfloor,$$
$$k_2 = \Big\lfloor \tfrac{\lambda - \frac{N}{3}(4^j-1) - 4^j i}{2^j}\Big\rfloor, \qquad k_1 = \lambda - \tfrac{N}{3}(4^j - 1) - 4^j i - 2^j k_2.$$

The indices $\lambda' = \theta(i, j+1, k')$ with $k' = (2k_1 + n, 2k_2 + n')$, $n, n' = 0, 1$, indicate the four sons of the element $\Gamma_{i,j,k}$.

For the sake of brevity we will write frequently Γ_λ instead of $\Gamma_{i,j,k}$. Moreover, it is rather convenient to set $|\lambda| := j$.

4.2 The wavelet representation

For each wavelet $\psi_{j,k}$ we introduce a set of elements $\mathcal{L}_{\psi_{j,k}}$ by the following convention. We first determine the set of coarse level elements

$$\mathcal{L}_{\psi_{j,k}}^{\text{coarse}} := \Big\{ \Gamma_{i,j,k'} \subseteq \operatorname{supp} \psi_{j,k} : \psi_{j,k}\big|_{\Gamma_{i,j,k'}} \in C^\infty(\Gamma_{i,j,k'}) \Big\}.$$

Clearly, we have $\bigcup_{\Gamma_\lambda \in \mathcal{L}_{\psi_{j,k}}^{\text{coarse}}} \Gamma_\lambda \subsetneq \operatorname{supp} \psi_{j,k}$. We now complete the support of the wavelet by the set of fine level elements

$$\mathcal{L}_{\psi_{j,k}}^{\text{fine}} := \Big\{ \Gamma_{i,j+1,k'} \subseteq \operatorname{supp} \psi_{j,k} : \bigcup_{\Gamma_\lambda \in \mathcal{L}_{\psi_{j,k}}^{\text{coarse}}} \Gamma_\lambda \cap \Gamma_{i,j+1,k'}^\circ = \emptyset \Big\}.$$

Thus, the union $\mathcal{L}_{\psi_{j,k}} := \mathcal{L}_{\psi_{j,k}}^{\text{coarse}} \cup \mathcal{L}_{\psi_{j,k}}^{\text{fine}}$ satisfies

$$\operatorname{supp} \psi_{j,k} = \bigcup_{\Gamma_\lambda \in \mathcal{L}_{\psi_{j,k}}} \Gamma_\lambda \subseteq \Omega_{j,k}, \qquad \Omega'_{j,k} \subseteq \bigcup_{\Gamma_\lambda \in \mathcal{L}_{\psi_{j,k}}} \partial\Gamma_\lambda. \tag{18}$$

Now, observing (7), for the piecewise constant wavelets we find unique weights $\omega_{\psi_{j,k}}^{\Gamma_\lambda} \in \mathbb{R}$ such that

$$\psi_{j,k}\big|_{\Gamma_\lambda} \equiv 2^{|\lambda|} \omega_{\psi_{j,k}}^{\Gamma_\lambda}, \qquad \Gamma_\lambda \in \mathcal{L}_{\psi_{j,k}}. \tag{19}$$

Likewise, via (8) and (9), for piecewise linear wavelets we obtain

$$\psi_{j,k}\big|_{\Gamma_\lambda}(x) = 2^{|\lambda|} \sum_{m=1}^{4} \omega_{m,\psi_{j,k}}^{\Gamma_\lambda} p_m^{\Gamma_\lambda}(s), \qquad x = \gamma_\lambda(s) \in \Gamma_\lambda, \qquad \Gamma_\lambda \in \mathcal{L}_{\psi_{j,k}} \tag{20}$$

with certain weights $\omega_{m,\psi_{j,k}}^{\Gamma_\lambda} \in \mathbb{R}$. This *element-based representation* is illustrated in Figure 3.

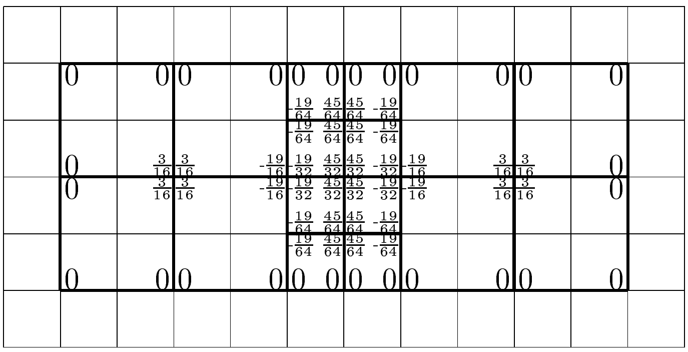

Figure 3: Element-based representation of a piecewise linear wavelet with four vanishing moments.

Remark: Storing all weights is expensive, particularly for the piecewise linears. Since many wavelets correspond to an identical mask, a suitable arrangement of the elements in the lists $\mathcal{L}_{\psi_{j,k}}$ induces identical lists of weights for such wavelets. Hence, we suggest to store only the different lists of weights. That way, the required memory is limited to $\mathcal{O}(1)$ since the number of different masks respective weights is independent of the level J.

4.3 The wavelet tree

In view of setting up the compression pattern, we introduce a wavelet tree defined with respect to the supports. Each wavelet has a certain number of sons with

$$\Omega_{j+1,\text{son}} \subseteq \Omega_{j,\text{father}}, \qquad \text{if } \psi_{j+1,\text{son}} \text{ is son of } \psi_{j,\text{father}}. \tag{21}$$

We mention that the father-son relation might be described by fixed index operations independently of the geometry. However, the tree depends on the chosen wavelet construction. Let us remark that the wavelet tree corresponds to the covering tree utilized for the *Panel Clustering*.

5 Computing distances numerically

To determine the degrees of quadrature it is required to evaluate the distance between elements. Additionally, for the matrix compression, the distance of the supports of wavelets as well as the distance of the singular support and the support of wavelets has to be computed.

5.1 Computing distances between elements

For each element Γ_λ we determine a sphere $B(m_{\Gamma_\lambda}, r_{\Gamma_\lambda}) := \big\{x \in \mathbb{R}^3 : \|x - m_{\Gamma_\lambda}\| \leq r_{\Gamma_\lambda}\big\}$ which encloses the element. Then, the distance between elements is approximated by

$$\begin{aligned} \operatorname{dist}(\Gamma_\lambda, \Gamma_{\lambda'}) &\geq \operatorname{dist}\big(B(m_{\Gamma_\lambda}, r_{\Gamma_\lambda}), B(m_{\Gamma_{\lambda'}}, r_{\Gamma_{\lambda'}})\big) \\ &= \max\{0, \|m_{\Gamma_\lambda} - m_{\Gamma_{\lambda'}}\| - r_{\Gamma_\lambda} - r_{\Gamma_{\lambda'}}\}. \end{aligned} \tag{22}$$

We start on the finest level $J = |\lambda|$ and compute the smallest sphere $B(m_{\Gamma_\lambda}, r_{\Gamma_\lambda})$ containing the four vertices of a given element Γ_λ. Assuming that J is sufficiently large, this sphere satisfies $\Gamma_\lambda \subseteq B(m_{\Gamma_\lambda}, r_{\Gamma_\lambda})$. Next, due to

$$\Gamma_\lambda = \bigcup_{\Gamma_{\lambda'} \text{ is son of } \Gamma_\lambda} \Gamma_{\lambda'},$$

the spheres to the elements on the lower levels are obtained recursively by determining the smallest spheres which contain the spheres of the associated sons. That way ensures $\Gamma_\lambda \in B(m_{\Gamma_\lambda}, r_{\Gamma_\lambda})$ for all $|\lambda| \leq J$ even if the surface Γ is strongly curved.

In the next subsection, the computation of the distance of the singular support and the support of wavelets is reduced to the computation of the distance $\operatorname{dist}(\Gamma_{i,j,k}, \partial\Gamma_{i',j',k'})$ $(j > j')$. Clearly, we find

$$\operatorname{dist}(\Gamma_{i,j,k}, \partial\Gamma_{i',j',k'}) = \operatorname{dist}(\Gamma_{i,j,k}, \Gamma_{i',j',k'}), \qquad i \neq i', \tag{23}$$

which is evaluated according to (22). Thus, it remains to consider $i = i'$. Since γ_i defines a diffeomorphism, we deduce

$$\operatorname{dist}(\Gamma_{i,j,k}, \partial\Gamma_{i,j',k'}) \sim \operatorname{dist}(\square_{j,k}, \partial\square_{j',k'}),$$

i.e. we might reduce our problem to the unit square. Observing that the l^2-norm and the l^∞-norm are equivalent in $\mathbb{R}^2$, the square $\square_{j,k}$ might be interpreted as the sphere $B(m_{\square_{j,k}}, r_{\square_{j,k}})$ with the midpoint $m_{\square_{j,k}} := \gamma_i\big(2^{-(j+1)}\big[\begin{smallmatrix}2k_1+1\\2k_2+1\end{smallmatrix}\big]\big)$ and the radius $r_{\square_{j,k}} := 2^{-(j+1)}$. Therefore, we conclude

$$\operatorname{dist}(\Gamma_{i,j,k}, \partial\Gamma_{i,j',k'}) \sim \big|\|m_{\square_{j,k}} - m_{\square_{j',k'}}\|_\infty - r_{\square_{j',k'}}\big| - r_{\square_{j,k}}, \tag{24}$$

where we utilized that either $\square_{j,k} \subseteq \square_{j',k'}$ or $\square_{j,k}^\circ \cap \square_{j',k'}^\circ = \emptyset$.

For each element, $\mathcal{O}(1)$ operations are performed to compute the midpoint and the radius of its enclosing sphere. Hence, observing that the number of elements is equal to $N_\Gamma \approx \frac{4}{3}N_J = \mathcal{O}(N_J)$, the complexity of computing and storing the midpoints and radii scales linearly with respect to the number of unknowns.

5.2 Computing distances between wavelets

Computing for each wavelet the sphere $B(m_{\psi_{j,k}}, r_{\psi_{j,k}})$ with

$$B(m_{\psi_{j,k}}, r_{\psi_{j,k}}) := \inf_{B(m,r)\in\mathbb{R}^3} \Big\{ B(m,r) \supseteq \bigcup_{\Gamma_\lambda \in \mathcal{L}_{\psi_{j,k}}} B(m_{\Gamma_\lambda}, r_{\Gamma_\lambda}) \Big\}$$

we conclude $\Omega_{j,k} \subseteq B(m_{\psi_{j,k}}, r_{\psi_{j,k}})$, cf. (18). Thus, the distance between the wavelets $\psi_{j,k}$ and $\psi_{j',k'}$ is computed analogously to (22) by

$$\operatorname{dist}(\Omega_{j,k}, \Omega_{j',k'}) \geq \max\{0, \|m_{\psi_{j,k}} - m_{\psi_{j',k'}}\| - r_{\psi_{j,k}} - r_{\psi_{j',k'}}\} \tag{25}$$

Clearly, the complexity of computing and storing all midpoints and radii of the enclosing spheres is $\mathcal{O}(N_J)$.

Next, the computation of $\operatorname{dist}(\Omega_{j,k}, \Omega'_{j',k'})$ is performed by invoking $\mathcal{L}_{\psi_{j,k}}$ and $\mathcal{L}_{\psi_{j',k'}}$. One readily infers

$$\operatorname{dist}(\Omega_{j,k}, \Omega'_{j',k'}) \gtrsim \min_{\Gamma_\lambda \in \mathcal{L}_{\psi_{j,k}}} \min_{\Gamma_{\lambda'} \in \mathcal{L}_{\psi_{j',k'}}} \big\{ \operatorname{dist}(\Gamma_\lambda, \partial\Gamma_{\lambda'}) \big\},$$

which is evaluated by (23) and (24), respectively.

6 Setting up the compression pattern

Checking the distance criteria (12) for each matrix coefficient, in order to assemble the compressed matrix, would require $\mathcal{O}(N_J^2)$ function calls. To realize linear complexity, we exploit the tree structure with respect to the supports of the wavelets, to predict negligible matrix coefficients. Recall that each son $\psi_{j+1,\text{son}}$ of the wavelet $\psi_{j,\text{father}}$ satisfies $\Omega_{j+1,\text{son}} \subseteq \Omega_{j,\text{father}}$. The following observation is an immediate consequence of the relations $\mathcal{B}_{j,j'} \ge \mathcal{B}_{j+1,j'} \ge \mathcal{B}_{j+1,j+1'}$, and $\mathcal{B}'_{j,j'} \ge \mathcal{B}'_{j+1,j'}$ for $j > j'$.

Lemma 6.1. *For $\Omega_{j+1,\text{son}} \subseteq \Omega_{j,\text{father}}$ and $\Omega_{j'+1,\text{son}} \subseteq \Omega_{j',\text{father}}$ the following statements hold.*

1. $\operatorname{dist}(\Omega_{j,\text{father}}, \Omega_{j',\text{father}'}) > \mathcal{B}_{j,j'}$ *implies* $\operatorname{dist}(\Omega_{j+1,\text{son}}, \Omega_{j',\text{father}'}) > \mathcal{B}_{j+1,j'}$ *as well as* $\operatorname{dist}(\Omega_{j+1,\text{son}}, \Omega_{j'+1,\text{son}'}) > \mathcal{B}_{j+1,j+1'}$.

2. *Suppose that $j > j'$ and* $\operatorname{dist}(\Omega_{j,\text{father}}, \Omega'_{j',\text{father}'}) > \mathcal{B}'_{j,j'}$. *Then one has* $\operatorname{dist}(\Omega_{j+1,\text{son}}, \Omega'_{j',\text{father}'}) > \mathcal{B}'_{j+1,j'}$.

With the aid of this lemma we have to check the distance criteria only for coefficients which stem from subdivisions of calculated coefficients on a coarser level. Therefore, the resulting procedure of checking the distance criteria is still of linear complexity. The subsequent algorithm computes the index sets $\mathcal{I}_{j,j'}$, $j_0 - 1 \le j, j' < J$, consisting of all index pairs (k, k') of relevant matrix coefficients. Note that the result of the function **relevant**$(\psi_{j,k}, \psi_{j',k'})$ is supposed to be **true**, if the matrix coefficient $\langle A\psi_{j',k'}, \psi_{j,k}\rangle$ is relevant according to (12). Otherwise it is **false**.

initialization: $\mathcal{I}_{j_0-1,j_0-1} := \{\Delta_{j_0} \times \Delta_{j_0}\}$; $\mathcal{I}_{j,j'} := \emptyset$ **elsewhere**
for $j := j_0$ **to** $J-1$ **do begin**
  for $j' := j_0 - 1$ **to** $j-1$ **do begin**
    for all $(\text{father}, \text{father}') \in \mathcal{I}_{j-1,j'}$ **do begin**   C: compute $\mathcal{I}_{j,j'}$ from $\mathcal{I}_{j-1,j'}$
      for all sons $\psi_{j,\text{son}}$ **of** $\psi_{j-1,\text{father}}$ **do begin**
        if $\big($**relevant**$(\psi_{j,\text{son}}, \psi_{j',\text{father}'}) =$ **true**$\big)$ $\mathcal{I}_{j,j'} := \mathcal{I}_{j,j'} \cup \{(\text{son}, \text{father}')\}$
    end; **end**
    $\mathcal{I}_{j',j} := \mathcal{I}_{j,j'}$ C: according to symmetry
  end
  for all $(\text{father}, \text{father}') \in \mathcal{I}_{j-1,j-1}$ **do begin**   C: compute $\mathcal{I}_{j,j}$ from $\mathcal{I}_{j-1,j-1}$
    for all sons $\psi_{j,\text{son}}$ **of** $\psi_{j-1,\text{father}}$ **do begin**
      for all sons $\psi_{j,\text{son}'}$ **of** $\psi_{j-1,\text{father}'}$ **do begin**
        if $\big($**relevant**$(\psi_{j,\text{son}}, \psi_{j,\text{son}'}) =$ **true**$\big)$ $\mathcal{I}_{j,j} := \mathcal{I}_{j,j} \cup \{(\text{son}, \text{son}')\}$
end; **end**; **end**; **end**

7 Assembling the system matrix

This section is concerned with the assemblation of the relevant matrix coefficients $\langle A\psi_{j',k'}, \psi_{j,k}\rangle$. For applying product Gauß quadrature rules it is required to split the wavelets into the smooth parts of their supports.

First, we consider piecewise constant wavelets. Invoking the wavelet representation (19) and abbreviating the *element-element interactions* by

$$\alpha_{\lambda,\lambda'} := 2^{|\lambda|+|\lambda'|} \int_{\square} \int_{\square} k\big(\gamma_\lambda(s), \gamma_{\lambda'}(t)\big) \kappa_\lambda(s) \kappa_{\lambda'}(t) dt ds, \tag{26}$$

we conclude

$$\langle A\psi_{j',k'}, \psi_{j,k}\rangle = \sum_{\Gamma_\lambda \in \mathcal{L}_{\psi_{j,k}}} \sum_{\Gamma_{\lambda'} \in \mathcal{L}_{\psi_{j',k'}}} \omega_{\psi_{j',k'}}^{\Gamma_{\lambda'}} \alpha_{\lambda,\lambda'}. \tag{27}$$

For piecewise linear wavelets, the element-element interactions are given by

$$\beta_{(m,\lambda),(m',\lambda')} := 2^{|\lambda|+|\lambda'|} \int_{\square} \int_{\square} k\big(\gamma_\lambda(s), \gamma_{\lambda'}(t)\big) p_m^{\square}(s) p_{m'}^{\square}(t) \kappa_\lambda(s) \kappa_{\lambda'}(t) dt ds. \tag{28}$$

Thus, the representation (20) yields the equation

$$\langle A\psi_{j',k'}, \psi_{j,k}\rangle = \sum_{\Gamma_\lambda \in \mathcal{L}_{\psi_{j,k}}} \sum_{\Gamma_{\lambda'} \in \mathcal{L}_{\psi_{j',k'}}} \sum_{m,m'=1}^{4} \omega_{m,\psi_{j,k}}^{\Gamma_\lambda} \omega_{m',\psi_{j',k'}}^{\Gamma_{\lambda'}} \beta_{(m,\lambda),(m',\lambda')}. \tag{29}$$

Consequently, the computation of the stiffness matrix is reduced to the computation of element-element interactions. But since, in general, the intersection of the supports of different wavelets is not empty, a naive calculation of (27) and (29) leads to a repeated computation of the element-element interactions. Hence, to develop an efficient algorithm, it is worth to examine these interactions.

8 On element-element interactions

As we have seen in the last section, the assembling of the compressed system matrix reduces to the computation of element-element interactions. Utilizing the mapping θ from (17), these element-element interactions are identified uniquely with coefficients of a (sparse) matrix $\mathbf{Q}_J$, where, in the case of piecewise linear wavelets, a single entry consists of 16 double values. The pattern of $\mathbf{Q}_J$ is structured similarly to the corresponding compressed system matrix, namely it is *finger structured*, cf. Figure 4.

Since nearly all element-element interactions of $\mathbf{Q}_J$ represent singular or nearly singular integrals, we often have to subdivide the associated domain of integration for quadrature. We realize this subdivision effectively by the following *recycling formulas* yielding again element-element interactions which can be *recycled* when assembling the compressed system

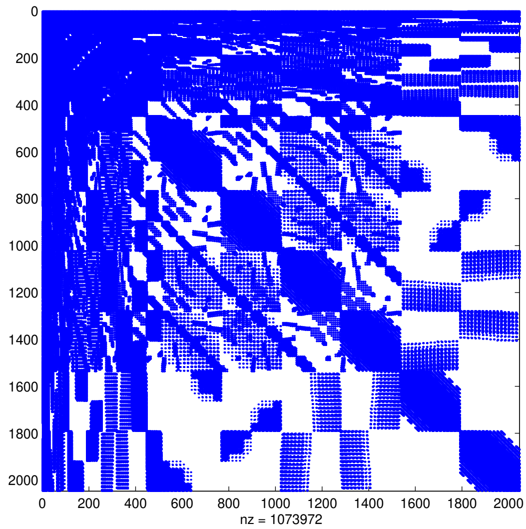

Figure 4: The matrix pattern of required element-element interactions.

matrix. Considering a given element Γ_{father} with index father $= (i, j, k)$, the indices of its sons are given by

$$\text{son}_1 := (i, j+1, (2k_1, 2k_2)), \qquad \text{son}_2 := (i, j+1, (2k_1+1, 2k_2)),$$
$$\text{son}_3 := (i, j+1, (2k_1, 2k_2+1)), \qquad \text{son}_4 := (i, j+1, (2k_1+1, 2k_2+1)).$$

In the case of piecewise constants, by (26) one readily verifies the recycling formulas

$$\begin{aligned} \alpha_{\text{father},\lambda} &= \tfrac{1}{2}\big[\alpha_{\text{son}_1,\lambda} + \alpha_{\text{son}_2,\lambda} + \alpha_{\text{son}_3,\lambda} + \alpha_{\text{son}_4,\lambda}\big], \\ \alpha_{\lambda,\text{father}} &= \tfrac{1}{2}\big[\alpha_{\lambda,\text{son}_1} + \alpha_{\lambda,\text{son}_2} + \alpha_{\lambda,\text{son}_3} + \alpha_{\lambda,\text{son}_4}\big]. \end{aligned} \tag{30}$$

Similar formulas can be derived in the case of piecewise linears, for example we have

$$\begin{aligned} &\beta_{(1,\text{father}),(m,\lambda)} = \tfrac{1}{2}\beta_{(1,\text{son}_1),(m,\lambda)} \\ &\quad+\tfrac{1}{4}\big[\beta_{(2,\text{son}_1),(m,\lambda)} + \beta_{(4,\text{son}_1),(m,\lambda)} + \beta_{(1,\text{son}_2),(m,\lambda)} + \beta_{(1,\text{son}_3),(m,\lambda)}\big] \\ &\quad+\tfrac{1}{8}\big[\beta_{(3,\text{son}_1),(m,\lambda)} + \beta_{(4,\text{son}_2),(m,\lambda)} + \beta_{(2,\text{son}_3),(m,\lambda)} + \beta_{(1,\text{son}_4),(m,\lambda)}\big], \\ &\beta_{(m,\lambda),(1,\text{father})} = \tfrac{1}{2}\beta_{(m,\lambda),(1,\text{son}_1)} \\ &\quad+\tfrac{1}{4}\big[\beta_{(m,\lambda),(2,\text{son}_1)} + \beta_{(m,\lambda),(4,\text{son}_1)} + \beta_{(m,\lambda),(1,\text{son}_2)} + \beta_{(m,\lambda),(1,\text{son}_3)}\big] \\ &\quad+\tfrac{1}{8}\big[\beta_{(m,\lambda),(3,\text{son}_1)} + \beta_{(m,\lambda),(4,\text{son}_2)} + \beta_{(m,\lambda),(2,\text{son}_3)} + \beta_{(m,\lambda),(1,\text{son}_4)}\big]. \end{aligned} \tag{31}$$

The pattern of $\mathbf{Q}_J$ is symmetric. This suggests to compute the element-element interaction of Γ_λ with $\Gamma_{\lambda'}$ and that of $\Gamma_{\lambda'}$ with Γ_λ simultaneously since the application of our quadrature algorithm yields many identical function calls.

Since a finite number of element-element interactions has to be calculated per relevant matrix coefficient, the number of nonzero coefficients of $\mathbf{Q}_J$ is $\mathcal{O}(N_J)$. However, storing $\mathbf{Q}_J$ completely is so expensive that the computable number of unknowns is restricted crucially.

Hence, we propose an element-based assembling of the system matrix. For a fixed index λ one computes and stores all required element-element interactions $\alpha_{\lambda,\lambda'}$ and $\alpha_{\lambda',\lambda}$ with $|\lambda| \geq |\lambda'|$, and likewise for the piecewise linears. Then, after updating the system matrix, these values can be deleted. Clearly, this strategy requires a rearrangement of the loops within the wavelet Galerkin scheme. But the number of multiple calculations is reduced enormously and the requirement of memory is limited to at most N_Γ element-element interactions.

9 Numerical integration

As we have seen in the previous sections it suffices to compute element-element interactions with respect to the domain of integration $\square \times \square$. Based on tensor product Gauß-Legendre rules we construct an adaptive quadrature algorithm which converges exponentially. In combination with Theorem 3.2 we realize linear complexity for the computation of the compressed system matrix.

9.1 Error estimates on the reference domain

For a given function $f \in L^2([0,1])$, we set $I^{[0,1]}f := \int_0^1 f(s)\, ds$. The g-point Gauß-Legendre formula on $[0,1]$ $Q_g^{[0,1]}f := \sum_{i=1}^g \omega_{g,i} f\big(\xi_{g,i}\big)$ applied to $f \in C^{2g}(0,1)$ can be estimated as

$$\big|R_g^{[0,1]}f\big| := \big|I^{[0,1]}f - Q_g^{[0,1]}f\big| \lesssim \frac{2^{-4g}}{(2g)!} \max_{s\in[0,1]} \big|f^{(2g)}(s)\big|, \tag{32}$$

cf. [18]. For $f \in L^2(\square)$ we define $I^\square f := \big(I^{[0,1]} \otimes I^{[0,1]}\big)f = \int_\square f(s)\, ds$ with $s = \big[\begin{smallmatrix} s_1 \\ s_2 \end{smallmatrix}\big]$. Approximating $I^\square f$ by the product Gauß-Legendre quadrature formula

$$Q_g^\square f := \big(Q_g^{[0,1]} \otimes Q_g^{[0,1]}\big)f = \sum_{i,i'=1}^{g} \omega_{g,i}\omega_{g,i'} f\big(\big[\begin{smallmatrix} \xi_{g,i} \\ \xi_{g,i'} \end{smallmatrix}\big]\big) \tag{33}$$

we find the following error estimate.

Lemma 9.1. *If $f \in C^{2g}(\square)$ the quadrature error $R_g^\square f := I^\square f - Q_g^\square f$ of the product Gauß-Legendre quadrature formula* (33) *is bounded by*

$$\big|R_g^\square f\big| \lesssim \frac{2^{-4g}}{(2g)!}\Big[\max_{s\in\square}\big|\partial_{s_1}^{2g} f(s)\big| + \max_{s\in\square}\big|\partial_{s_2}^{2g} f(s)\big|\Big]. \tag{34}$$

Proof. Invoking (32), the classical tensor product argument

$$\begin{aligned} R_g^\square f &= \Big[\big(I^{[0,1]} \otimes I^{[0,1]}\big) - \big(Q_g^{[0,1]} \otimes Q_g^{[0,1]}\big)\Big]f \\ &= \Big[\big(I^{[0,1]} \otimes I^{[0,1]}\big) - \big(I^{[0,1]} \otimes Q_g^{[0,1]}\big) + \big(I^{[0,1]} \otimes Q_g^{[0,1]}\big) - \big(Q_g^{[0,1]} \otimes Q_g^{[0,1]}\big)\Big]f \\ &= \Big[I^{[0,1]} \otimes \big(I^{[0,1]} - Q_g^{[0,1]}\big)\Big]f + \Big[\big(I^{[0,1]} - Q_g^{[0,1]}\big) \otimes Q_g^{[0,1]}\Big]f \end{aligned}$$

leads us to the desired estimate (34). $\square$

Next, to a function $f(s,t) \in L^2(\square \times \square)$ we apply the four dimensional product Gauß-Legendre quadrature formula

$$Q_{g,g'}^{\square\times\square} f := \big(Q_g^{\square} \otimes Q_{g'}^{\square}\big) f = \sum_{i,i'=1}^{g} \sum_{j,j'=1}^{g'} \omega_{g,i}\omega_{g,i'}\omega_{g',j}\omega_{g',j'} f\big(\big[\begin{smallmatrix}\xi_{g,i}\\ \xi_{g,i'}\end{smallmatrix}\big], \big[\begin{smallmatrix}\xi_{g',j}\\ \xi_{g',j'}\end{smallmatrix}\big]\big) \tag{35}$$

in order to approximate the integral $I^{\square\times\square} f := \big(I^{\square} \otimes I^{\square}\big) f = \int_{\square}\int_{\square} f(s,t)\, dt\, ds$.

Lemma 9.2. *For $f(s,t) \in C^{2g}(\square) \times C^{2g'}(\square)$ the quadrature error $R_{g,g'}^{\square\times\square} f := I^{\square\times\square} f - Q_{g,g'}^{\square\times\square} f$ of the product Gauß-Legendre quadrature formula* (35) *can be estimated by*

$$\begin{aligned} \big|R_{g,g'}^{\square\times\square} f\big| \lesssim & \frac{2^{-4g}}{(2g)!}\Big[\max_{s,t\in\square}\big|\partial_{s_1}^{2g} f(s,t)\big| + \max_{s,t\in\square}\big|\partial_{s_2}^{2g} f(s,t)\big|\Big] \\ & + \frac{2^{-4g'}}{(2g')!}\Big[\max_{s,t\in\square}\big|\partial_{t_1}^{2g'} f(s,t)\big| + \max_{s,t\in\square}\big|\partial_{t_2}^{2g'} f(s,t)\big|\Big]. \end{aligned}$$

Proof. This lemma is proved analogously to the latter lemma. $\square$

9.2 Basic estimates

We now assume that the diffeomorphisms γ_i are analytical on $\square$ for all $i \in \{1, 2, \ldots, M\}$. Then, in general, a given boundary integral operator $A : H^q(\Gamma) \to H^{-q}(\Gamma)$ of order $2q$ satisfies the following definition.

Definition 9.3. *A kernel $k(x,y)$ is called analytically standard of order $2q$, if the partial derivatives of the transported kernel functions* (6) *are bounded by*

$$|\partial_s^{\alpha}\partial_t^{\beta} k_{i,i}(s,t)| \lesssim \|\gamma_i(s), \gamma_{i'}(t)\|^{-(2+2q+|\alpha|+|\beta|)},$$

with some $r > 0$, provided that $2 + 2q + |\alpha| + |\beta| > 0$.

Defining the local transported kernels

$$k_{\lambda,\lambda'}(s,t) := k\big(\gamma_\lambda(s), \gamma_{\lambda'}(t)\big)\kappa_\lambda(s)\kappa_{\lambda'}(t) dt ds$$

for $s, t \in \square$, we find the relation

$$I^{\square\times\square} k_{\lambda,\lambda'} = 2^{-(|\lambda|+|\lambda'|)}\alpha_{\lambda,\lambda'}. \tag{36}$$

Lemma 9.4. *Let the kernel $k(x,y)$ be analytically standard of order $2q$ and assume that* $\operatorname{dist}(\Gamma_\lambda, \Gamma_{\lambda'}) > 0$. *Then, applying the quadrature formula $Q_{g,g'}^{\square\times\square}$ defined in* (35) *to the integral* (36) *yields the error estimate*

$$\begin{aligned} \big|R_{g,g'}^{\square\times\square} k_{\lambda,\lambda'}\big| \lesssim 2^{-2(|\lambda|+|\lambda|')} \Bigg[& \left(\frac{2^{-|\lambda|}}{4r}\right)^{2g} \operatorname{dist}(\Gamma_\lambda, \Gamma_{\lambda'})^{-(2+2q+2g)} \\ & + \left(\frac{2^{-|\lambda'|}}{4r}\right)^{2g'} \operatorname{dist}(\Gamma_\lambda, \Gamma_{\lambda'})^{-(2+2q+2g')}\Bigg]. \end{aligned} \tag{37}$$

Proof. Since the kernel is analytically standard of order $2q$, the equations (4) and (5) imply the estimate

$$|\partial_s^\alpha \partial_t^\beta k_{\lambda,\lambda'}(s,t)| \lesssim \frac{(|\alpha|+|\beta|)!}{r^{|\alpha|+|\beta|}} \frac{2^{-|\lambda|(|\alpha|+2)}2^{-|\lambda'|(|\beta|+2)}}{\big\|\gamma_\lambda(s)-\gamma_{\lambda'}(t)\big\|^{2+2q+|\alpha|+|\beta|}} \tag{38}$$

Hence, we find

$$\begin{aligned}\max_{s,t\in\square}\big|\partial_{s_n}^{2g} k_{\lambda,\lambda'}(s,t)\big| &\lesssim 2^{-2(|\lambda|+|\lambda'|)}\ 2^{-2g|\lambda|}\ \frac{(2g)!}{r^{2g}}\ \min_{s,t\in\square}\big\|\gamma_\lambda(s)-\gamma_{\lambda'}(t)\big\|^{-(2+2q+2g)}\\ &\lesssim 2^{-2(|\lambda|+|\lambda'|)}\ 2^{-2g|\lambda|}\ \frac{(2g)!}{r^{2g}}\ \operatorname{dist}(\Gamma_\lambda,\Gamma_{\lambda'})^{-(2+2q+2g)}\end{aligned}$$

for $n=1,2$. Analogously one infers

$$\max_{s,t\in\square}\big|\partial_{t_n}^{2g'} k_{\lambda,\lambda'}(s,t)\big| \lesssim 2^{-2(|\lambda|+|\lambda'|)}\ 2^{-2g'|\lambda'|}\ \frac{(2g')!}{r^{2g'}}\ \operatorname{dist}(\Gamma_\lambda,\Gamma_{\lambda'})^{-(2+2q+2g')}.$$

The integrand $k_{\lambda,\lambda'}$ is nonsingular if $\operatorname{dist}(\Gamma_\lambda,\Gamma_{\lambda'})>0$. Therefore, we conclude the desired estimate by Lemma 9.2. $\square$

In the case of piecewise linear wavelets, we have to compute in accordance with (28) the integrals

$$I^{\square\times\square}\big[k_{\lambda,\lambda'}(p_m^\square\otimes p_{m'}^\square)\big] = 2^{-(|\lambda|+|\lambda'|)}\beta_{(m,\lambda),(m',\lambda')}. \tag{39}$$

Herein, $p_m^\square$, $p_{m'}^\square$ denote the bilinear polynomials on $\square$ defined by (8).

Lemma 9.5. *Let the kernel $k(x,y)$ be analytically standard of order $2q$ and assume that $\operatorname{dist}(\Gamma_\lambda,\Gamma_{\lambda'})\gtrsim 2^{-\min\{|\lambda|,|\lambda'|\}}$. Then, the application of the quadrature formula $Q_{g,g'}^{\square\times\square}$ (35) to the integral (39) yields the error estimate*

$$\begin{aligned}\big|R_{g,g'}^{\square\times\square}\big[k_{\lambda,\lambda'}(p_m^\square\otimes p_{m'}^\square)\big]\big| \lesssim& \left(\frac{2^{-|\lambda|}}{4r}\right)^{2g}\frac{2^{-2|\lambda|'-|\lambda|}}{\operatorname{dist}(\Gamma_\lambda,\Gamma_{\lambda'})^{1+2q+2g}}\\ &+\left(\frac{2^{-|\lambda'|}}{4r}\right)^{2g'}\frac{2^{-2|\lambda|-|\lambda|'}}{\operatorname{dist}(\Gamma_\lambda,\Gamma_{\lambda'})^{1+2q+2g'}}.\end{aligned} \tag{40}$$

Proof. The $(2g)$-th partial derivative of $k_{\lambda,\lambda'}(s,t)p_m^\square(s)p_{m'}^\square(t)$ with respect to s_n, $n=1,2$, is given by

$$\begin{aligned}\partial_{s_n}^{2g}\big[k_{\lambda,\lambda'}(s,t)p_m^\square(s)p_{m'}^\square(t)\big] =& \partial_{s_n}^{2g}k_{\lambda,\lambda'}(s,t)p_m^\square(s)p_{m'}^\square(t)\\ &+\partial_{s_n}^{2g-1}k_{\lambda,\lambda'}(s,t)\partial_{s_n}p_m^\square(s)p_{m'}^\square(t).\end{aligned}$$

Obviously, there holds $\left|p_m^\square(s)p_{m'}^\square(t)\right| \le 1$ and $\left|\frac{\partial p_m^\square(s)}{\partial s_n}p_{m'}^\square(t)\right| \le 1$ for all $s,t \in \square$ and $1 \le m,m' \le 4$, cf. (8). Therefore, according to (38) we find the bound

$$\begin{aligned}
&\max_{s,t\in\square}\left|\partial_{s_n}^{2g}\left[k_{\lambda,\lambda'}(s,t)p_m^\square(s)p_{m'}^\square(t)\right]\right.\\
&\quad\lesssim 2^{-2g|\lambda|}\frac{(2g)!}{r^{2g}}\frac{2^{-2|\lambda'|-|\lambda|}}{\operatorname{dist}(\Gamma_\lambda,\Gamma_{\lambda'})^{1+2q+2g}}\underbrace{\left[\frac{2^{-|\lambda|}}{\operatorname{dist}(\Gamma_\lambda,\Gamma_{\lambda'})}+\frac{r}{2g}\right]}_{\lesssim 1 \text{ since } \operatorname{dist}(\Gamma_\lambda,\Gamma_{\lambda'})\gtrsim 2^{-\min\{|\lambda|,|\lambda'|\}}}\\
&\quad\lesssim 2^{-2g|\lambda|}\frac{(2g)!}{r^{2g}}\frac{2^{-2|\lambda'|-|\lambda|}}{\operatorname{dist}(\Gamma_\lambda,\Gamma_{\lambda'})^{1+2q+2g}}.
\end{aligned}$$

Analogously one gets the corresponding result for the derivatives with respect to t_1 and t_2. Hence, (40) is valid according to Lemma 9.2. $\square$

We now can formulate the following proposition which is an immediate consequence of the Lemmata 9.4 and 9.5.

Proposition 9.6. *Let the kernel $k(x,y)$ be analytically standard of order $2q$ and ε denote a given precision. Consider two elements Γ_λ and $\Gamma_{\lambda'}$ which satisfy the distance criterion*

$$\operatorname{dist}(\Gamma_\lambda,\Gamma_{\lambda'}) \ge 2^{-\min\{|\lambda|,|\lambda'|\}}s, \qquad s > \frac{1}{4r}. \tag{41}$$

Choosing the degrees of quadrature

$$\begin{aligned}
g &= \left\lceil -\tfrac{1}{2}\cdot\tfrac{|\lambda|+|\lambda'|+\log_2(\varepsilon)+(2+2q)\log_2(\operatorname{dist}(\Gamma_\lambda,\Gamma_{\lambda'}))}{|\lambda|+2+\log_2 r+\log_2(\operatorname{dist}(\Gamma_\lambda,\Gamma_{\lambda'}))}\right\rceil,\\
g' &= \left\lceil -\tfrac{1}{2}\cdot\tfrac{|\lambda|+|\lambda'|+\log_2(\varepsilon)+(2+2q)\log_2(\operatorname{dist}(\Gamma_\lambda,\Gamma_{\lambda'}))}{\lambda'|+2+\log_2 r+\log_2(\operatorname{dist}(\Gamma_\lambda,\Gamma_{\lambda'}))}\right\rceil,
\end{aligned}\tag{42}$$

in the case of piecewise constant wavelets and

$$\begin{aligned}
g &= \left\lceil -\tfrac{1}{2}\cdot\tfrac{|\lambda'|+\log_2\varepsilon+(1+2q)\log_2(\operatorname{dist}(\Gamma_\lambda,\Gamma_{\lambda'}))}{|\lambda|+2+\log_2 r+\log_2(\operatorname{dist}(\Gamma_\lambda,\Gamma_{\lambda'}))}\right\rceil,\\
g' &= \left\lceil -\tfrac{1}{2}\cdot\tfrac{|\lambda|\ +\log_2\varepsilon+(1+2q)\log_2(\operatorname{dist}(\Gamma_\lambda,\Gamma_{\lambda'}))}{|\lambda'|+2+\log_2 r+\log_2(\operatorname{dist}(\Gamma_\lambda,\Gamma_{\lambda'}))}\right\rceil,
\end{aligned}\tag{43}$$

in the case of piecewise linear wavelets, the Gauß-Legendre quadrature formula $Q_{g,g'}^{\square\times\square}$ (35) computes the element-element interaction $\alpha_{\lambda,\lambda'}$ or $\beta_{(m,\lambda),(m',\lambda')}$ with precision $\sim\varepsilon$.

Notice that the error of quadrature does not tend to zero when increasing g and g' if the elements violate the distance criterion (41). For such integrals we propose an adaptive quadrature strategy in the next subsection.

A special situation occurs if $|\lambda| = |\lambda'|$ and $\Gamma_\lambda \cap \Gamma_{\lambda'} \neq \emptyset$, i.e., if both elements are identical or share a common edge or vertex. Then, the domain of integration contains the singularity. We utilize the *Duffy trick* to transform the singular integrands on nonsingular ones, cf. [15, 27, 28]. It turns out, that the error of quadrature behaves like in (37) and (40), respectively, with $\text{dist}(\Gamma_\lambda, \Gamma_{\lambda'}) := 2^{-|\lambda|}$. Consequently, we have to subdivide the domain of integration $[0,1]^4$ into 16^m same sized cubes. Herein, m denotes the nonnegative integer $m := \max\{0, \lceil \log_2 s \rceil\}$ with s from (41). After rescaling the domains of integration to $[0,1]^4$, the application of the quadrature formula $Q_{g,g'}^{\square\times\square}$ with

$$g = g' = \left\lceil \tfrac{q|\lambda| - (\log_2 \varepsilon)/2}{2+m+\log_2 r} \right\rceil. \tag{44}$$

yields a quadrature error $\lesssim \varepsilon$. We like to mention that we are allowed to choose $s = 1$ if $r > 1/4$. Then, no subdivision ($m = 0$) is required and the degrees of quadrature coincide with those of (42) and (43) when setting $\text{dist}(\Gamma_\lambda, \Gamma_{\lambda'}) = 2^{-|\lambda|}$.

9.3 An adaptive quadrature strategy

We are now in the position to formulate the adaptive algorithm. It is defined recursively and stops after a finite number of steps. The algorithm performs the computation of a the element-element interaction of Γ_λ with $\Gamma_{\lambda'}$ with the precision ε. Without loss of generality we assume $|\lambda| \geq |\lambda'|$. An example of the subdivision of the elements is depicted in Figure 5. Note that, when we compute a desired element-element interaction by the recycling formulas, the quadrature error appears four times. Therefore, observing the weight factors of the element-element interactions, the precision of quadrature has to be increased to $\varepsilon/2$ to claim the precision ε.

1. *Starting point.* If the elements Γ_λ and $\Gamma_{\lambda'}$ violate the distance criterion (41) then goto item *2* if $|\lambda| > |\lambda'|$ and goto item *3* if $|\lambda| = |\lambda'|$. Otherwise apply the product Gauß-Legendre quadrature formula $Q_{g,g'}^{\square\times\square}$ choosing g and g' as in proposition 9.6.

2. *Case* $|\lambda| > |\lambda'|$. Replace the larger element Γ_λ by its four sons and compute the associated element-element interactions with precision $\varepsilon/2$ according to item *1*. The desired element-element interaction is calculated via the recycling formulas.

3. *Case* $|\lambda| > |\lambda'|$. If the domain of integration contains the singularity then apply the Duffy trick. Else, replace the element $\Gamma_{\lambda'}$ by its four sons and compute the associated element-element interactions with precision $\varepsilon/2$ according to item *1*. The desired element-element interaction is calculated via the recycling formulas.

Since the support of a wavelet on the level j os subdivided into finitely many elements of the levels j and $j+1$, it suffices to compute the element-element interactions of Γ_λ and $\Gamma_{\lambda'}$ with the precision $\varepsilon_{|\lambda|,|\lambda'|}$ according to (3.3).

The recycling can be realized easily by inserting the line "return the previously computed element-element interaction if it exists" in item *1*. According to

$$\varepsilon_{j,j'} \leq \varepsilon_{j+1,j'} \leq \varepsilon_{j+1,j'+1}, \qquad j_0 - 1 \leq j \leq j' < J - 1,$$

cf. (16), this requires the element-element interactions computed successively by starting on the coarse grid.

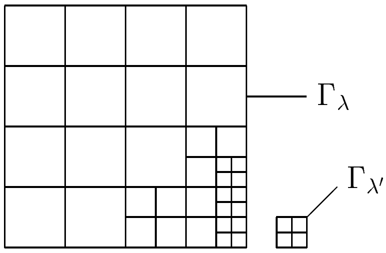

Figure 5: This subdivision of the elements Γ_λ and $\Gamma_{\lambda'}$ results if $s = 3/2$.

The next theorem proves in combination with Theorem 3.2 that the proposed quadrature strategy computes in fact the compressed system matrix in linear complexity. This is achieved even without the recycling of previously computed element-element interactions. But we emphasize that the recycling accelerates the computation of the system matrix enormously.

Theorem 9.7. *Exploiting the adaptive quadrature algorithm introduced above, the computation of the element-element interactions $\alpha_{\lambda,\lambda'}$ and $\beta_{(m,\lambda),(m',\lambda')}$ with the precision $\varepsilon_{j,j'}$ given by* (16) *requires $\mathcal{O}\big(\big[J+1-\frac{|\lambda|+|\lambda'|}{2}\big]^4\big)$ operations.*

Proof. i. Due to (13) we find $\frac{d'-q}{\tilde{d}+q} < 1$. Consequently, $\varepsilon_{j,j'}$ can be estimated by

$$\varepsilon_{j,j'} \sim \underbrace{\min\left\{2^{-|j-j'|}, 2^{-2(J-\frac{j+j'}{2})\frac{d'-q}{\tilde{d}+q}}\right\}}_{\geq 2^{-2(J-\frac{j+j'}{2})}} 2^{2Jq}2^{-2d'(J-\frac{j+j'}{2})} \geq 2^{2Jq}2^{-2(d'+1)(J-\frac{j+j'}{2})}.$$

Moreover, according to (35), the quadrature rule $Q_{g,g'}^{\square\times\square}$ applies $(gg')^2$ quadrature knots. The evaluation of the recycling formulas scales linearly with the number of computed element-element interactions. For the sake of simplicity, in the sequel we restrict ourselves to piecewise constant wavelets. The desired result for the piecewise linear wavelets is confirmed in complete analogy.

ii. First, we consider the case that the associated elements Γ_λ and $\Gamma_{\lambda'}$ satisfy the distance criterion (41). Without loss of generality we assume $|\lambda'| \geq |\lambda|$ which implies $\operatorname{dist}(\Gamma_\lambda, \Gamma_{\lambda'}) \geq 2^{-|\lambda|}s$ and $g \geq g'$. In particular, we have

$$|\lambda| + 2 + \log_2 r + \log_2\big(\operatorname{dist}(\Gamma_\lambda, \Gamma_{\lambda'})\big) \geq |\lambda| + 2 + \log_2 r + \log_2(2^{-|\lambda|}s) =: c_s > 0.$$

Inserting this inequaliy into (42) yields

$$\begin{aligned} g' \leq g &\sim -\tfrac{1}{2}\cdot\frac{|\lambda|+|\lambda'|+\log_2(\varepsilon_{|\lambda|,|\lambda'|})+(2+2q)\log_2(\operatorname{dist}(\Gamma_\lambda,\Gamma_{\lambda'}))}{|\lambda|+2+\log_2 r+\log_2(\operatorname{dist}(\Gamma_\lambda,\Gamma_{\lambda'}))} \\ &\leq -\tfrac{1}{2c_s}\big[|\lambda|+|\lambda'|+\log_2(\varepsilon_{|\lambda|,|\lambda'|})+(2+2q)\log_2(2^{-|\lambda|}s)\big] \\ &\leq \tfrac{1}{2c_s}\big[|\lambda|-|\lambda'|-2q(J-|\lambda|)+(2d'+1)\big(J-\tfrac{|\lambda|+|\lambda|'}{2}\big)+(2+2q)\log_2(1/s)\big]. \end{aligned}$$

Due to

$$|\lambda| - |\lambda'| - 2q(J - |\lambda|) \le \begin{cases} -2q\big(J - \frac{|\lambda|+|\lambda|'}{2}\big), & \text{if } q \ge -1, \\ -4q\big(J - \frac{|\lambda|+|\lambda|'}{2}\big), & \text{otherwise,} \end{cases}$$

we conclude $g' \le g \lesssim J + 1 - \frac{|\lambda|+|\lambda|'}{2}$. This proves the assertion due to item *i*.

iii. Next, we treat the case that $|\lambda| = |\lambda'|$ and $\Gamma_\lambda \cap \Gamma_{\lambda'} \neq \emptyset$, i.e. the Duffy trick is applied. We have to compute 16^m, $m = \max\{0, \lceil \log_2 s \rceil\}$, integrals with the degree of quadrature given by (44). We find $2 + m + \log_2 r \ge c_s$ which implies

$$\begin{aligned} g = g' &\sim \tfrac{q|\lambda| - (\log_2 \varepsilon_{|\lambda|,|\lambda'|})/2}{2+m+\log_2 r} \le \tfrac{1}{c_s}\big[q|\lambda| - Jq + (d'+1)\big(J - \tfrac{|\lambda|+|\lambda'|}{2}\big)\big] \\ &= \tfrac{d'+1-q}{c_s}\big(J - \tfrac{|\lambda|+|\lambda'|}{2}\big) \lesssim J - \tfrac{|\lambda|+|\lambda'|}{2}. \end{aligned}$$

In fact, the complexity is $\mathcal{O}\big(\big[J + 1 - \frac{|\lambda|+|\lambda'|}{2}\big]^4\big)$ since $m \sim 1$ independently of $|\lambda|$ and J.

iv. We consider again $|\lambda| = |\lambda'|$ and two disjoint elements Γ_λ and $\Gamma_{\lambda'}$ which violate the distance criterion (41). Since the mesh is quasi uniform, a constant $c_\Gamma > 0$ exists such that $\operatorname{dist}(\Gamma_\lambda, \Gamma_{\lambda'}) \ge 2^{-|\lambda|} c_\Gamma$ for all pairs of elements with $\Gamma_\lambda \cap \Gamma_{\lambda'} = \emptyset$. Herein, c_Γ depends only on the manifold and its parametrization but not on $|\lambda|$ or J. The algorithm subdivides the desired element-element interaction in at most 16^m element-element interactions $\alpha_{\widehat{\lambda},\widehat{\lambda}'}$, with $|\widehat{\lambda}| = |\widehat{\lambda}'| = |\lambda| + m$ and $m = \max\{0, \lceil \log_2(s/c_\Gamma) \rceil\}$. Thereby, the precision $\varepsilon_{|\lambda|,|\lambda|'}$ is increased to $2^{-2m}\varepsilon_{|\lambda|,|\lambda|'}$. Due to

$$|\lambda| + m + 2 + \log_2 r + \log_2 \underbrace{\big(\operatorname{dist}(\Gamma_{\widehat{\lambda}}, \Gamma_{\widehat{\lambda}'})\big)}_{\ge \operatorname{dist}(\Gamma_\lambda, \Gamma_{\lambda'}) \ge 2^{-|\lambda|} c_\Gamma} \ge c_s$$

the degrees of quadrature are estimated by

$$\begin{aligned} g = g' &\sim -\tfrac{1}{2} \cdot \tfrac{|\lambda|+|\lambda'|+2m+\log_2(2^{-2m}\varepsilon_{|\lambda|,|\lambda'|})+(2+2q)\log_2(\operatorname{dist}(\Gamma_{\widehat{\lambda}},\Gamma_{\widehat{\lambda}'}))}{|\lambda|+m+2+\log_2 r+\log_2(\operatorname{dist}(\Gamma_{\widehat{\lambda}},\Gamma_{\widehat{\lambda}'}))} \\ &\quad - \tfrac{1}{2c_\Gamma}\big[|\lambda| + |\lambda'| + \log_2(\varepsilon_{|\lambda|,|\lambda'|}) + (2+2q)\log_2(2^{-|\lambda|}c_\Gamma)\big] \lesssim J + 1 - \tfrac{|\lambda|+|\lambda'|}{2} \end{aligned}$$

analogously to item *ii*. Again, the complexity is $\mathcal{O}\big(\big[J - \frac{|\lambda|+|\lambda|'}{2}\big]^4\big)$ since $m \sim 1$ independently of $|\lambda|$ and J.

v. Finally, we consider the case of two elements Γ_λ and $\Gamma_{\lambda'}$, $|\lambda'| \neq |\lambda|$, violating the distance criterion (41). Without loss of generality we assume $|\lambda'| > |\lambda|$. Moreover, we make use of the following observation. Due to $\operatorname{diam}(\Gamma_{\widehat{\lambda}}) \sim 2^{-|\widehat{\lambda}|}$, for a fixed level $|\widehat{\lambda}| \le |\lambda'|$, only $\mathcal{O}(s^2)$ elements $\Gamma_{\widehat{\lambda}}$ are found with $\operatorname{dist}(\Gamma_{\widehat{\lambda}}, \Gamma_\lambda) < s2^{-|\widehat{\lambda}|}$. Consequently, our algorithm subdivides for all $|\lambda| < |\widehat{\lambda}| \le |\lambda'|$ only $\mathcal{O}(s^2)$ element-element interactions while $\mathcal{O}(s^2)$ element-element interactions are evaluated since they satisfy the distance criterion.

Thus, on the level $|\widehat{\lambda}|$, we compute $\mathcal{O}(s^2)$ element-element interactions satisfying

$$\operatorname{dist}(\Gamma_{\widehat{\lambda}}, \Gamma_{\lambda'}) \ge 2^{-|\widehat{\lambda}|}s = 2^{-|\lambda|}2^{|\lambda|-|\widehat{\lambda}|}s,$$

with the precision $2^{|\lambda|-|\widehat{\lambda}|}\varepsilon_{|\lambda|,|\lambda'|}$. The degree of quadrature for the element larger element is bounded by

$$
\begin{aligned}
g &\sim -\tfrac{1}{2}\cdot\tfrac{|\widehat{\lambda}|+|\lambda'|+\log_2(2^{|\lambda|-|\widehat{\lambda}|}\varepsilon_{|\lambda|,|\lambda'|})+(2+2q)\log_2(\operatorname{dist}(\Gamma_{\widehat{\lambda}},\Gamma_{\lambda'}))}{|\widehat{\lambda}|+2+\log_2 r+\log_2(\operatorname{dist}(\Gamma_{\widehat{\lambda}},\Gamma_{\lambda'}))}\\
&\le -\tfrac{1}{2c_s}\big\{\big[|\lambda|+|\lambda'|+\log_2(\varepsilon_{|\lambda|,|\lambda'|})+(2+2q)\log_2(2^{-|\lambda|}s)\big]+(2+2q)(|\lambda|-|\widehat{\lambda}|)\big\}
\end{aligned}
$$

Herein, the first term is bounded by

$$
-\tfrac{1}{2c_s}\big[|\lambda|+|\lambda'|+\log_2(\varepsilon_{|\lambda|,|\lambda'|})+(2+2q)\log_2(2^{-|\lambda|}s)\big]\lesssim J-\tfrac{|\lambda|+|\lambda'|}{2}
$$

according to item *ii* while the second term satisfies

$$
\frac{1+q}{c_s}(|\widehat{\lambda}|-|\lambda|)\le\begin{cases}\frac{2+2q}{c_s}(J-\frac{|\lambda|-|\lambda'|}{2}), & \text{if } q\ge -1,\\ 0, & \text{otherwise,}\end{cases}
$$

This implies $g\lesssim J+1-\frac{|\lambda|-|\lambda'|}{2}$ and

$$
\begin{aligned}
g' &\sim -\tfrac{1}{2}\cdot\tfrac{|\widehat{\lambda}|+|\lambda'|+\log_2(2^{|\lambda|-|\widehat{\lambda}|}\varepsilon_{|\lambda|,|\lambda'|})+(2+2q)\log_2(\operatorname{dist}(\Gamma_{\widehat{\lambda}},\Gamma_{\lambda'}))}{|\lambda|'+2+\log_2 r+\log_2(\operatorname{dist}(\Gamma_{\widehat{\lambda}},\Gamma_{\lambda'}))}\\
&= -\tfrac{1}{2}\cdot\tfrac{|\widehat{\lambda}|+|\lambda'|+\log_2(2^{|\lambda|-|\widehat{\lambda}|}\varepsilon_{|\lambda|,|\lambda'|})+(2+2q)\log_2(\operatorname{dist}(\Gamma_{\widehat{\lambda}},\Gamma_{\lambda'}))}{[|\lambda'|-|\widehat{\lambda}|]+[|\widehat{\lambda}|+2+\log_2 r+\log_2(\operatorname{dist}(\Gamma_{\widehat{\lambda}},\Gamma_{\lambda'}))]}\\
&\lesssim \tfrac{1}{|\lambda'|-|\widehat{\lambda}|+c_s}\big(J+1-\tfrac{|\lambda|+|\lambda'|}{2}\big).
\end{aligned}
$$

Consequently, $\mathcal{O}\big(\frac{1}{(|\lambda'|-|\widehat{\lambda}|+c_s)^2}\big[J-\frac{|\lambda|+|\lambda'|}{2}\big]^4\big)$ quadrature knots are applied. Now, we sum over $\widehat{j}$ with $j:=|\lambda|<\widehat{j}\le|\lambda'|=:j'$ and obtain

$$
\sum_{\widehat{j}=j+1}^{j'}\frac{1}{(j'-\widehat{j}+c_s)^2}<\sum_{\widehat{j}=0}^{\infty}\frac{1}{(\widehat{j}+c_s)^2}<\frac{1}{c_s^2}+\sum_{\widehat{j}=1}^{\infty}\frac{1}{\widehat{j}^2}=\frac{1}{c_s^2}+\frac{\pi^2}{6}\lesssim 1.
$$

Consequently, we find the complextity $\mathcal{O}\big(\big[J+1-\frac{|\lambda|+|\lambda'|}{2}\big]^4\big)$ of computing all element-element interactions $\alpha_{\widehat{\lambda},\lambda'}$ with $|\widehat{\lambda}|\ge|\lambda'|$.

The complexity of computing the remaining $\mathcal{O}(s^2)$ element-element interactions $\alpha_{\widehat{\lambda},\lambda'}$, $|\widehat{\lambda}|=|\lambda'|$, with the precision $2^{|\lambda|-|\lambda'|}\varepsilon_{|\lambda|,|\lambda'|}\ge 2^{-2(J-\frac{|\lambda|+|\lambda'|}{2})}\varepsilon_{|\lambda|,|\lambda'|}$ is also $\mathcal{O}\big(\big[J+1-\frac{|\lambda|+|\lambda'|}{2}\big]^4\big)$ which is verified analogously to the items *iii* and *iv*. This finishes the proof. □

10 Numerical results

In order to demonstrate the efficiency of our method we present in this section some numerical results. We choose our problem such that the solution is known analytically. We consider the Laplace equation

$$
\Delta u = 0 \quad in\Omega
$$

where we choose Ω as the gearwheel presented in Figure 1. Choosing the Dirichlet data $f := u\big|_\Gamma$ or Neumann data $g := \partial u/partialn$ of the harmonical function $u(x) = \langle x, b\rangle/\|x\|^3$, $x \notin \Omega$, then u is the unique solution (modulo some constant in the case of the Neumann problem) of the interior Dirichlet and Neumann problem, respectively.

We solve these both, the interior Dirichlet and Neumann problem, by the indirect approach using the *single layer operator*

$$V : H^{-1/2}(\Gamma) \to H^{1/2}(\Gamma), \qquad (V\rho)(x) = \int_\Gamma \frac{1}{\|x-y\|}\rho(y)d\sigma_y,$$

the *double layer operator* K and its adjoint $K^\star$

$$K : L^2(\Gamma) \to L^2(\Gamma), \qquad (K\rho)(x) = \int_\Gamma \frac{\partial}{\partial n_y}\frac{1}{\|x-y\|}\rho(y)d\sigma_y,$$
$$K^\star : L^2(\Gamma) \to L^2(\Gamma), \qquad (K^\star\rho)(x) = \int_\Gamma \frac{\partial}{\partial n_x}\frac{1}{\|x-y\|}\rho(y)d\sigma_y,$$

as well as the hypersingular operator

$$W : H^{+1/2}(\Gamma) \to H^{-1/2}(\Gamma), \qquad (W\rho)(x) = -\frac{\partial}{\partial n_x}\int_\Gamma \frac{\partial}{\partial n_y}\frac{1}{\|x-y\|}\rho(y)d\sigma_y.$$

The indirect method yields a density ρ living on the boundary Γ which leads to the solution $u(x)$ by potential evaluation. More precisely, the Dirichlet problem we derive the Fredholm integral equations of the first kind

$$V\rho = f \text{ on } \Gamma, \qquad u(x) = (V\rho)(x) \text{ in } \Omega, \tag{45}$$

and of the second kind

$$(K - \tfrac{1}{2})\rho = f \text{ on } \Gamma, \qquad u(x) = (K\rho)(x) \text{ in } \Omega. \tag{46}$$

The Neumann problem is solved via the Fredholm integral equations of the first kind

$$W\rho = g \text{ on } \Gamma, \qquad u(x) = (K\rho)(x) \text{ in } \Omega, \tag{47}$$

and of the second kind

$$(K^\star + \tfrac{1}{2})\rho = g \text{ on } \Gamma, \qquad u(x) = (V\rho)(x) \text{ in } \Omega. \tag{48}$$

We solve all these integral equations using piecewise constant and bilinear wavelets. Equations (45), (46), and (48) are discretized by by piecewise constant wavelets with three vanishing moments as well as piecewise bilinear wavelets with double nodes along the interfaces and four vanishing moments. The discretization of (47) requires *globally continuous* piecewise bilinear wavelet bases since the energy space of the hypersingular operator is $H^{1/2}(\Gamma)$. It suffices that these wavelets provide two vanishes moments.

Problem	J	N_J	$\|\mathbf{u}-\mathbf{u}_J\|_\infty$	cpu-time (sec.)	density (%)
Equation (45)	1	1344	5.94e-1	10	15
discretized by	2	5376	4.94e-2 (12)	27	4.7
piecewise constant	3	21504	2.62e-2 (1.9)	308	1.7
wavelets	4	86016	5.25e-3 (5.0)	2339	0.55
Equation (46)	1	1344	2.89	3	15
discretized by	2	5376	1.43e-1 (20)	26	3.8
piecewise constant	3	21504	4.37e-2 (3.3)	257	1.3
wavelets	4	86016	1.15e-2 (3.8)	1610	0.37
Equation (45)	1	3024	1.44e-2	35	100
discretized by	2	8400	7.34e-3 (2.0)	111	16
piecewise bilinear	3	27216	3.72e-3 (2.0)	1366	4.1
wavelets	4	97104	8.61e-5 (43)	12185	1.3
Equation (46)	1	3024	3.42e-1	27	100
discretized by	2	8400	1.35e-1 (2.5)	105	16
piecewise bilinear	3	27216	1.70e-2 (7.9)	1424	3.5
wavelets	4	97104	1.71e-3 (9.9)	12992	0.95

Table 1: Numerical results for the Dirichlet problem.

Problem	J	N_J	$\|\mathbf{u}-\mathbf{u}_J\|_\infty$	cpu-time (sec.)	density (%)
Equation (48)	1	1344	6.25e-1	3	15
discretized by	2	5376	5.99e-1 (1.0)	26	3.8
piecewise constant	3	21504	7.18e-2 (8.3)	257	1.3
wavelets	4	86016	2.78e-2 (2.6)	1610	0.37
Equation (47)	1	1344	7.89e-1	19	100
discretized by	2	5376	5.08e-1 (1.6)	469	18
piecewise bilinear	3	21504	3.62e-2 (14)	3137	5.1
wavelets	4	86016	6.13e-3 (5.9)	16247	1.4
Equation (48)	1	3024	6.44e-1	27	100
discretized by	2	8400	2.44e-1 (2.6)	105	16
piecewise bilinear	3	27216	7.50e-3 (33)	1424	3.5
wavelets	4	97104	6.46e-3 (1.2)	12992	0.95

Table 2: Numerical results for the Neumann problem.

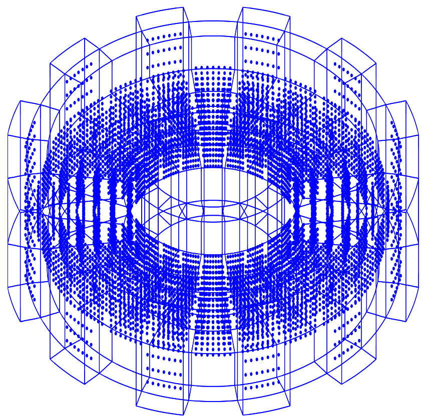

Figure 6: The evaluation points of the solution.

The approximate solution u_J is computed in a lot of points x_i distributed in the interior of the gearwheel as shown in Figure 6. Depending on the approximation order d and the operator order $2q$, the optimal order of convergence of the maximum norm of the absolute errors $u(x_i) - u_J(x_i)$ is given by $\|\mathbf{u} - \mathbf{u}_J\|_\infty \lesssim 2^{-2J(d-q)}$ if the density ρ is sufficiently smooth, cf. [32]. We mention that this order cannot be expected due to reentrant edges of our geometry.

We perform the computation by a standard personal computer with 1 Gigabyte main memory. In the Tables 1 and 2 we tabulated the results for the Dirichlet and the Neumann problem, respectively. The cpu-time refers to the computation of the approximate density, i.e. assembling and solving the linear system of equations. The number of nonzero coefficients of the system matrix (density) is given in percent. The density versus the number of unknowns is visualized in Figure 7. One figures out that the number of nonzero coefficients tends in fact to a linear scaling (dashed line). In Figure 8 we plot the absolute error versus the cpu-time. In the case of the Dirichlet problem (left plot), one observes that the single layer operator yields the best performance. In the case of the Neumann problem (right plot), the adjoint of the double layer operator discretized by piecewise bilinears is the best choice. We emphasize that only two levels are computable by the traditional Galerkin scheme. Its accuracy is nearly identical to that of the wavelet Galerkin scheme.

References

[1] G. Beylkin, R. Coifman, and V. Rokhlin. The fast wavelet transform and numerical algorithms. *Comm. Pure and Appl. Math.*, 44:141–183, 1991.

[2] C. Canuto, A. Tabacco, and K. Urban. The wavelet element method, part I: Construction and analysis. *Appl. Comput. Harm. Anal.*, 6:1–52, 1999.

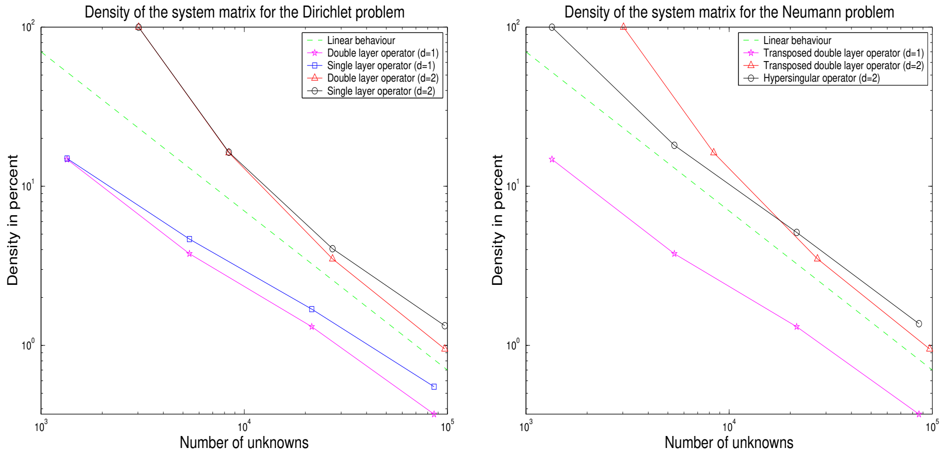

Figure 7: Compression rates for the Dirichlet (left) and Neumann (right) problem.

[3] A. Cohen, I. Daubechies, and J.-C. Feauveau. Biorthogonal bases of compactly supported wavelets. *Pure Appl. Math.*, 45:485–560, 1992.

[4] A. Cohen and R. Masson. Wavelet adaptive method for second order elliptic problems – boundary conditions and domain decomposition. *Numer. Math.*, 86:193–238, 2000.

[5] W. Dahmen. Wavelet and multiscale methods for operator equations. *Acta Numerica*, 6:55–228, 1997.

[6] W. Dahmen, H. Harbrecht and R. Schneider. Compression techniques for boundary integral equations – optimal complexity estimates. *Preprint SFB 393/02-06, TU Chemnitz*, 2002. submitted to SIAM J. Numer. Anal.

[7] W. Dahmen and A. Kunoth. Multilevel preconditioning. *Numer. Math.*, 63:315–344, 1992.

[8] W. Dahmen, B. Kleemann, S. Prößdorf, and R. Schneider. A multiscale method for the double layer potential equation on a polyhedron. In H.P. Dikshit and C.A. Micchelli, editors, *Advances in Computational Mathematics*, pages 15–57, World Scientific Publ., Singapore, 1994.

[9] W. Dahmen, A. Kunoth, and K. Urban. Biorthogonal spline-wavelets on the interval – stability and moment conditions. *Appl. Comp. Harm. Anal.*, 6:259–302, 1999.

[10] W. Dahmen, S. Prößdorf, and R. Schneider. Wavelet approximation methods for periodic pseudodifferential equations. Part II – Fast solution and matrix compression. *Advances in Computational Mathematics*, 1:259–335, 1993.

[11] W. Dahmen, S. Prößdorf, and R. Schneider. Multiscale methods for pseudodifferential equations on smooth manifolds. In C.K. Chui, L. Montefusco, and L. Puccio, editors,

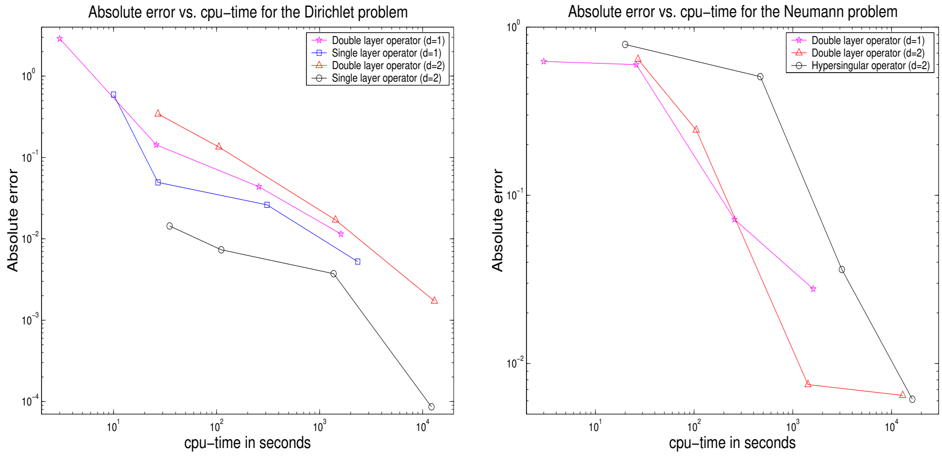

Figure 8: Performance with respect to the Dirichlet (left) and to the Neumann (right) problem.

Proceedings of the International Conference on Wavelets: Theory, Algorithms, and Applications, pages 385–424, 1995.

[12] W. Dahmen and R. Schneider. Composite wavelet bases for operator equations. *Math. Comp.*, 68:1533–1567, 1999.

[13] W. Dahmen and R. Schneider. Wavelets on manifolds I. Construction and domain decomposition. *SIAM J. Math. Anal.*, 31:184–230, 1999.

[14] W. Dahmen and R. Stevenson. Element-by-element construction of wavelets satisfying stability and moment conditions. *SIAM J. Numer. Anal.*, 37:319–352, 1999.

[15] M. Duffy. Quadrature over a pyramid or cube of integrands with a singularity at the vertex. *SIAM J. Numer. Anal.*, 19:1260–1262, 1982.

[16] L. Greengard and V. Rokhlin. A fast algorithm for particle simulation. *J. Comput. Phys.*, 73:325–348, 1987.

[17] W. Hackbusch and Z.P. Nowak. On the fast matrix multiplication in the boundary element method by panel clustering. *Numer. Math.*, 54:463–491, 1989.

[18] G. Hämmerlin and K.-H. Hoffmann. *Numerische Mathematik*. Springer-Verlag, Berlin-Heidelberg, 1992. 3. Auflage.

[19] H. Harbrecht. Wavelet Galerkin schemes for the boundary element method in three dimensions. *PHD Thesis, Technische Universität Chemnitz, Germany*, 2001.

[20] H. Harbrecht, F. Paiva, C. Pérez, and R. Schneider. Biorthogonal wavelet approximation for the coupling of FEM-BEM. *Preprint SFB 393/99-32, TU Chemnitz*, 1999. to appear in Numer. Math.

[21] H. Harbrecht, F. Paiva, C. Pérez, and R. Schneider. Wavelet preconditioning for the coupling of FEM-BEM. *Preprint SFB 393/00-07, TU Chemnitz*, 2000. to appear in Numerical Linear Algebra with Applications.

[22] Y. Meyer. *Ondelettes et Opérateurs 2: Opérateur de Caldéron-Zygmund.* Hermann, Paris 1990.

[23] J.-C. Nedelec. *Acoustic and Electromagnetic Equations - Integral Representations for Harmonic Problems.* Springer Verlag, 2001.

[24] T. von Petersdorff, R. Schneider, and C. Schwab. Multiwavelets for second kind integral equations. *SIAM J. Num. Anal.*, 34:2212–2227, 1997.

[25] T. von Petersdorff and C. Schwab. Fully discretized multiscale Galerkin BEM. In W. Dahmen, A. Kurdila, and P. Oswald, editors, *Multiscale wavelet methods for PDEs*, pages 287–346, Academic Press, San Diego, 1997.

[26] A. Rathsfeld. A quadrature algorithm for wavelet Galerkin methods. In *Über Waveletalgorithmen für die Randelementmethode.* Habilitation Thesis, Technische Universität Chemnitz, Germany, 2001.

[27] S. Sauter. Über die effiziente Verwendung des Galerkin Verfahrens zur Lösung Fredholmscher Integralgleichungen. *PHD Thesis, Christian–Albrecht–Universität Kiel, Germany*, 1992.

[28] S. Sauter and C. Schwab. Quadrature for the *hp*-Galerkin BEM in $\mathbb{R}^3$. *Numer. Math.*, 78:211–258, 1997.

[29] R. Schneider. *Multiskalen- und Wavelet-Matrixkompression: Analysisbasierte Methoden zur Lösung großer vollbesetzter Gleichungssysteme.* B.G. Teubner, Stuttgart, 1998.

[30] C. Schwab. Variable order composite quadrature of singular and nearly singular integrals. *Computing*, 53:173–194, 1994.

[31] L. Villemoes. Wavelet analysis of refinement equations. *SIAM J. Math. Anal.*, 25:1433–1460, 1994.

[32] W.L. Wendland, On asymptotic error analysis and underlying mathematical principles for boundary element methods. In C.A. Brebbia, editor, *Boundary Element Techniques in Computer Aided Engineering, NATO ASI Series E - 84*, pages 417–436, Martinus Nijhoff Publ., Dordrecht-Boston-Lancaster, 1984.